OPEN ACCESS Freely available online

PLoS GENETICS

Repeated, Selection-Driven Genome Reduction of Accessory Genes in Experimental Populations

Ming-Chun Lee[1¤], **Christopher J. Marx**[1,2*]

1 Department of Organismic and Evolutionary Biology, Harvard University, Cambridge, Massachusetts, United States of America, **2** Faculty of Arts and Sciences Center for Systems Biology, Harvard University, Cambridge, Massachusetts, United States of America

Abstract

Genome reduction has been observed in many bacterial lineages that have adapted to specialized environments. The extreme genome degradation seen for obligate pathogens and symbionts appears to be dominated by genetic drift. In contrast, for free-living organisms with reduced genomes, the dominant force is proposed to be direct selection for smaller, streamlined genomes. Most variation in gene content for these free-living species is of "accessory" genes, which are commonly gained as large chromosomal islands that are adaptive for specialized traits such as pathogenicity. It is generally unclear, however, whether the process of accessory gene loss is largely driven by drift or selection. Here we demonstrate that selection for gene loss, and not a shortened genome, per se, drove massive, rapid reduction of accessory genes. In just 1,500 generations of experimental evolution, 80% of populations of *Methylobacterium extorquens* AM1 experienced nearly parallel deletions removing up to 10% of the genome from a megaplasmid present in this strain. The absence of these deletion events in a mutation accumulation experiment suggested that selection, rather than drift, has dominated the process. Reconstructing these deletions confirmed that they were beneficial in their selective regimes, but led to decreased performance in alternative environments. These results indicate that selection can be crucial in eliminating unnecessary genes during the early stages of adaptation to a specialized environment.

Citation: Lee M-C, Marx CJ (2012) Repeated, Selection-Driven Genome Reduction of Accessory Genes in Experimental Populations. PLoS Genet 8(5): e1002651. doi:10.1371/journal.pgen.1002651

Editor: Nancy A. Moran, Yale University, United States of America

Received November 3, 2011; **Accepted** February 28, 2012; **Published** May 10, 2012

Funding: This work was funded by a grant from the NSF (DEB-0845893). The funders had no role in study design, data collection and analysis, decision to publish, or preparation of the manuscript.

Competing Interests: The authors have declared that no competing interests exist.

* E-mail: cmarx@oeb.harvard.edu

¤ Current address: Department of Biochemistry, The University of Hong Kong, Pokfulam, Hong Kong

Introduction

Bacterial genomes have the potential to rapidly change their size and content as a result of various mechanisms such as deletion, duplication and horizontal gene transfer. The net expansion or contraction at the genome scale is thus a function of both the rate at which these events occur and the subsequent filters imposed by natural selection and/or genetic drift [1,2]. Although most bacterial genomes have remained relatively constant in size due to an apparent overall balance of these forces [3], distinct strains within a species can differ remarkably in gene content [4]. This finding has led to categorizing the genome into the core and accessory (or auxiliary) components, the former being present in nearly all members, and the latter being present in only a subset of strains [5].

The population biology and selective environment of microbes each contribute to the tempo and mode of genomic change. Of primary importance is the effective population size (N_e) of a species, as this influences the efficacy of selection versus drift. Repeated bottlenecks, such as those experienced by intracellular endosymbionts (which also participate in little, if any horizontal gene transfer), result in tremendous rates of sequence change and ineffective selection to maintain functions required for host-independent lifestyle. This often leads to loss of many genes that are essential for the free-living microbes and massive genome shrinkage (ex: 77% in the intracellular symbiont of aphids, *Buchnera aphidicola* and genomes as small as *Hodgkinia cicadicola* (144 kb)) [2,6–9]. On the other hand, simply living on a restricted set of resources in a relatively constant environment can also result in reduced genomes despite very large N_e, such as observed for the plankton *Prochlorococcus* and *Pelagibacter* [10,11]. For these it has been suggested that the major force driving genome reduction is streamlining, defined as when "selection acts to reduce genome size because of the metabolic burden of replicating DNA with no adaptive value" [11]. In addition to DNA synthesis, deletions also eliminate producing the RNA molecules and proteins encoded by that region.

Beyond external factors, the genomic structure of microbes and mechanisms of gene gain and loss make it possible for large regions to come and go in single events. Accessory genes are disproportionately found on extrachromosomal replicons that are subject to potential loss. Alternatively, even when present on the main chromosome accessory genes are often found as discrete genomic islands disrupting an otherwise syntenic chromosome between strains in a species. This can result in gains or losses via various mechanisms such as homologous or site-specific recombination and phage integration/excision [12], resulting in punctuated large-scale gene content changes. Large-scale reductions of accessory genomes via these events may be a critical mechanism in early stages of genome shrinkage.

Although either drift or selection could contribute to genome reduction observed in nature, we lack direct evidence to distinguish between the lack of purifying selection to maintain

Author Summary

Many free-living bacteria are known to commonly lose large portions of their genomes, but it is unclear what evolutionary forces drive these changes. Is this due to random loss in small populations, as is thought to be the case for the extreme genome degradation of intracellular symbionts, or due to selection? And if it is beneficial, is it directly caused by replicating a shorter genome or advantageous loss of the genes themselves? We uncovered that most replicate populations of *Methylobacterium extorquens* AM1 evolved in the laboratory for 1,500 generations lost nearly 10% of their genome. Through reconstructing these deletions, we demonstrated that these losses were indeed beneficial, but the advantage did not scale with length of genome lost, and were even deleterious in alternative environments. These findings suggest that the initial stages of genome shrinkage may be driven by selection, ultimately leading to a more streamlined, specialized organism.

the genes lost versus positive selection for their loss. Genomic analyses of chronic infections, such as *Pseudomonas aeruginosa* in cystic fibrosis patients, have repeatedly observed large deletions [13–15]. This rapid loss of genomic islands could simply be due to high rates of recombination and drift (or hitchhiking). Alternatively, the instability of the accessory genome could be due to selection, either for reduced genome length (*i.e.*, streamlining) or beneficial gene loss, such as has been shown for *Shigella flexneri*, a facultative intracellular pathogen of primates [16].

Laboratory-evolved populations of bacteria present the unique opportunity to address the forces involved in genome reduction under selective regimes that tilt the relative efficacy of selection versus drift. 'Mutation accumulation' experiments purposefully use single-colony bottlenecks at each transfer to maximize drift [17]. In contrast, the more typical experimental evolution regimes maintain an N_e often in the millions, allowing selection to dominate [18,19]. To date, genome reductions found in the above experiments have tended to be modest (up to 4% of the genome in mutation accumulation experiments, and 1% in larger populations). The DNA loss rates observed have been low ($\sim$2 bp per generation), and the regions lost have largely been inconsistent across lineages. With the exception of small (1.6–7 kb) deletions in the ribose gene cluster of *Escherichia coli* [20], none of these genome reductions have been tested for their fitness effects. As such, it remains unclear whether these observed genome reductions imparted an advantage in the selective environment, whether fitness effects scale with the length of DNA removed, and/or whether such events generate tradeoffs across other environments.

Here, we used experimental evolution to investigate the role of large-scale deletions in adaptation and specialization. We evolved populations of the α-proteobacterium *Methylobacterium extorquens* AM1, a member of the dominant genera found on leaf surfaces [21,22]. Like other bacteria that utilize single-carbon (C_1) compounds (*e.g.*, methanol) as growth substrates, *M. extorquens* AM1 has also specialized to grow on a very limited array of multi-C compounds (*e.g.*, succinate), and has been a model for exploring rapid metabolic specialization during adaptation [22]. Across 32 populations evolved for 1500 generations in one of four different nutrient regimes we found 80% of these deleted the same genomic region that encompasses up to 10% of the genome. By reconstructing these deletions under the ancestral genetic background we have demonstrated that they rose in frequency due to selection; however, the advantage gained was not a generic effect of shortening genome length, but was specific to the region lost and imparted an advantage (or disadvantage) that depended upon the environment.

Results/Discussion

Adaptation of populations and identification of massive, parallel deletions

In order to examine the potential role of large-scale deletions in adaptation of *M. extorquens* AM1 we analyzed genome content from replicate evolved populations. Eight parallel populations were grown at a large N_e ($\sim 2.5\times10^8$) in each of four different nutrient regimes (32 populations in total): methanol, succinate, mixture of methanol and succinate, or alternating between methanol and succinate. After 1500 generations, the evolved populations increased fitness in their selective environments by 15 to 37% compared to their wild-type ancestor (Figure S1). As reported previously [22], a couple of these strains were actually less fit than the ancestor, which likely represent genotypes that exist due to frequency-dependent interactions such as cross-feeding. For comparison, we also maintained 10 lineages on solid medium for 1500 generations that we transferred through single-cell bottlenecks to maximize the strength of drift.

To determine the extent to which large-scale deletions contributed to adaptation, we used comparative genomic hybridization (CGH) to uncover chromosomal changes in 44 isolates from the 32 evolved populations (Table S1). Like many bacteria, the 6.9 Mb genome of *M. extorquens* AM1 has multiple replicons of varying sizes (5.5 Mb chromosome, 1.3 Mb megaplasmid present at one copy per chromosome, and 3 plasmids between 25–44 kb present between 1–3 copies per chromosome) [23], a total of 23 distinct deletions were identified, some of which in more than one lineage (Table S2). Over 91% of the deletion events were due to homologous recombination between matching sequence regions, and of these, 86% were between co-directional pairs of one of the 142 insertion sequences (ISs) present in the genome of *M. extorquens* AM1 [23]. Most notable were the extensive, repeated changes to the megaplasmid: 36 of the 44 isolates screened by CGH contained deletions spanning a single region that ranged from 23 kb to 641 kb (Figure 1A). The largest of these deletions removed 24.7% of the accessory genes (unique to *M. extorquens* AM1 versus strain DM4) [23] and 2.7% of shared, core genes. This represents the largest parallel losses observed during laboratory adaptation thus far. Previous experiments either observed an occasional large deletion (200 kb) [17] or repeated loss of small regions ($<$7 kb) [20]. Applying a PCR-based screen to 56 additional isolates revealed 51 more with deletions in this region (Table S1). Despite this overall parallelism, the precise borders of these deletions were somewhat different. We broadly classified these into three classes of deletion types (DT1, 2, and 3; Figure 1A). A DT1 event with borders precisely at a co-directional pair of ISs had been independently identified by genome re-sequencing of a methanol-evolved isolate from a population initiated with a different starting genotype [24]. These deletion types were present at significantly different proportions across the four nutrient regimes (Figure 1B). Moreover, since distinct subtypes of deletions coexisted in some populations at changing frequencies (Figure 1B and Text S1), the larger deletions may have occurred stepwise, as proposed for similar events in the genomes of *B. aphidicola* strains [25].

Large-scale deletions were beneficial in the selective environments they arose

The observed parallelism across replicates could be due to either an unusually high rate of occurrence and/or a selective advantage

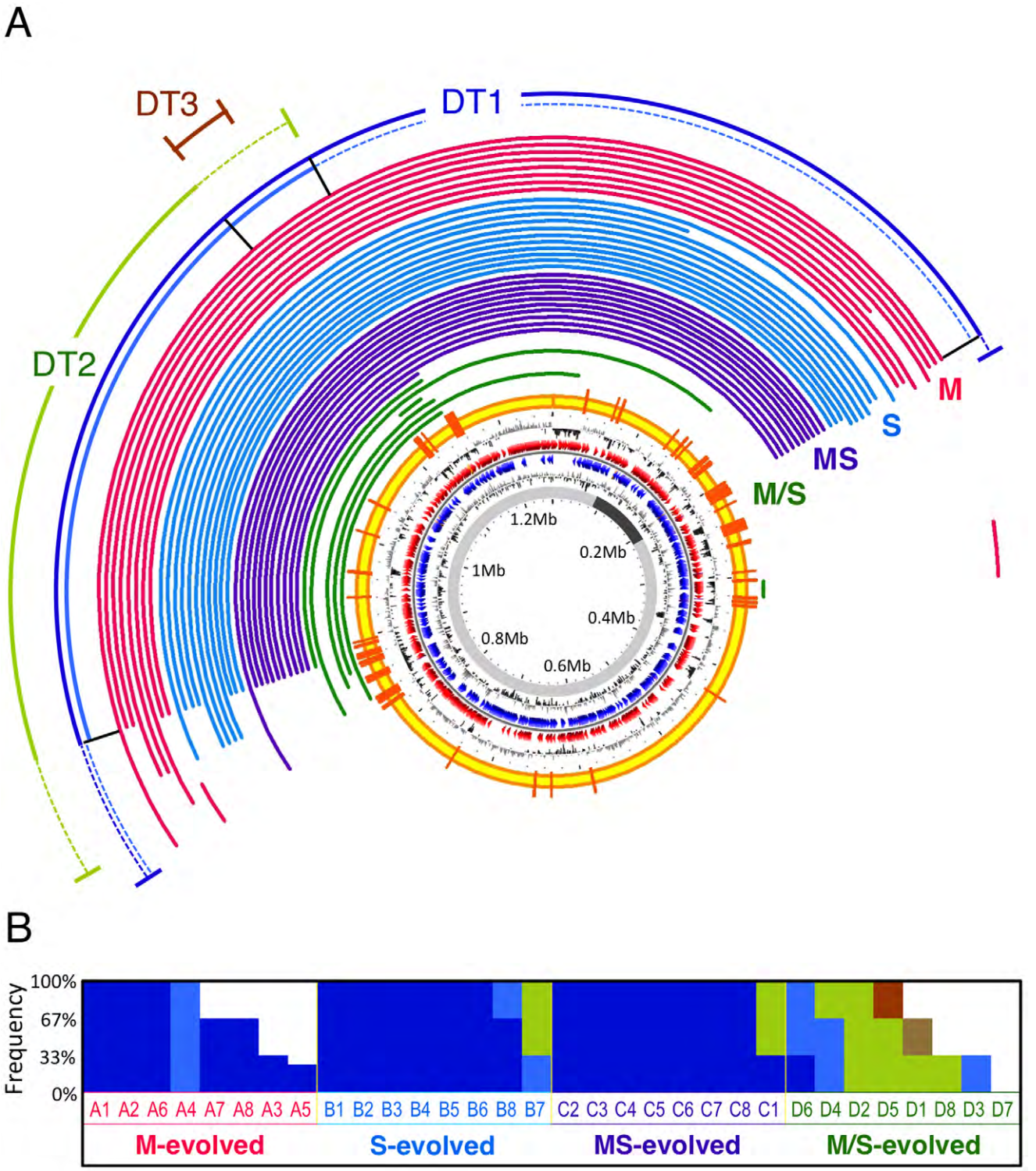

Figure 1. Parallel deletions on megaplasmid found in evolved isolates. (A) Deletions detected by CGH arrays. Each arc represents the deleted region in an isolate with the color indicating the selective environment: pink, M (methanol); blue, S (succinate); purple, MS (methanol+succinate); green, M/S (alternating methanol/succinate). Observed deletion types (DT1, 2, and 3) were classified by PCR detection using 4 pairs of primers in region R1, R2, R3 or R4 (black bars from left to right) and are shown as the outside arcs with dashed lines indicating the ranges of edges for subtypes. DT1a: all 4 pairs gave negative results (dark blue). DT1b: R1, R2, and R3 negative R4 positive (light blue). DT2: R1 and R2 came back negative but R3 and R4 were positive (light green). DT3a: only one isolate had this deletion, which was detected by the arrays (brown). DT3b: R1, R2 and R4 came back positive but R3 was negative (not shown in Figure 1A). (Methods, Tables S1 and S3). Successive circles from inside to outside: conserved region in *M. extorquens* DM4 and CM4 (dark grey), GC skew, predicted CDSs transcribed in the counterclockwise direction (blue), predicted CDSs in clockwise direction (red), GC% deviation, IS position (orange bar). (B) Frequency of deletion types in isolates from populations. Three or four isolates were obtained in each population (labeled columns sorted by number and type of deletions for clarity) and their deletion type is indicated by color: DT1a, dark blue; DT1b, light blue; DT2, light green; DT3a, brown; DT3b, light brown.
doi:10.1371/journal.pgen.1002651.g001

conferred by the events themselves. For example, the parallel deletions of regions of the ribose operon of glucose-evolved *E. coli* were shown to partly depend upon a high rate of transposition and subsequent recombination [20]. To address this possibility, we examined the 10 populations transferred through single-colony bottlenecks for 1500 generations. None of the defined deletion types were detected by PCR, which is significantly unlikely to be observed given the rate they appeared in the large N_e populations ($P<0.0001$) (Text S1).

In order to directly test for a possible selective advantage of these deletions, we reconstructed deletions in the wild-type ancestor and tested whether these were individually beneficial in their selective environments. We created four deletions that represent the largest class found (engineered type 1, ET1), the half of ET1 that was commonly lost (ET2), a small region, itself only observed once, at the intersection of all identified deletions (ET3), and a fourth region (ET4) that, although never observed to be lost in the evolved populations, removed the alternative half of DT1 and was equivalent in length to ET2 (both ~300 kb) (Figure 2A). With the exception of ET3 in the methanol/succinate switching environment, all deletion types were individually beneficial in the selective environments that they were observed in, with up to a 15% selective advantage for ET1 in succinate medium (Figure 2B). The nearly neutral fitness effect of ET3 indicated that the beneficial effect was not due to removing this shared region. Interestingly, the fitness effect of ET1 was approximately the same as expected from the two half deletions (ET2 and ET4), suggesting that there is little epistasis between these two regions (Figure S2 and Text S1).

The selective advantage of gene loss is not due to a shorter genome and leads to tradeoffs in alternative environments

Two lines of evidence refuted the hypothesis that the physiological basis of the fitness advantage of the large-scale deletions was simply due to a shorter genome, and rather suggested that loss of specific gene(s) was the primary benefit. The streamlining hypothesis that genome reduction is driven by metabolic efficiency of a shorter genome would predict that: 1) the magnitude of benefit would scale with size of the deletion and 2) the benefit would be reasonably similar across multiple environments. First, we found that selective advantage did not correlate with deletion size. This is most clearly demonstrated by comparing ET2 and ET4, which have equivalent lengths. These two ~300 kb deletions exert quite different effects, whereas ET1 (which is twice as large) and ET4 behaved quite similarly. Second, we found that, although the marginal benefits of ET2 and ET3 were relatively constant across different growth substrates, but the phenotype of ET1 and ET4 varied markedly. This included being a disadvantage during growth on methanol when transferred from succinate, which appears to be due to a longer transition time between nutrients and decreased fitness during stationary phase on succinate (Figure 2C, 2D and Figure S3). This result is in consistent with a recent report where no correlation between genome size and selection intensity was found across a variety of natural isolated bacteria [26]. The high prevalence of observing DT1 in populations evolved in succinate and the methanol-succinate mixture is in accord with the above phenotypes, but other factors such as epistatic interactions with previous mutations

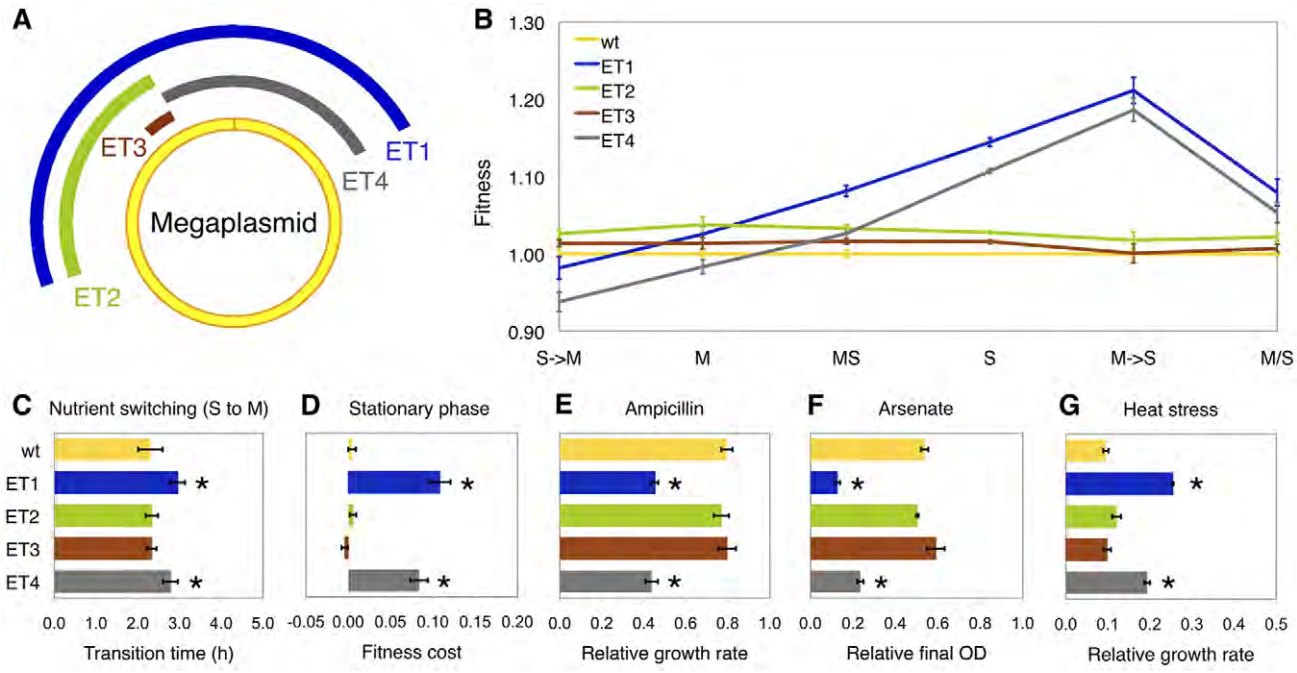

Figure 2. Phenotypes of deletion mutants. (A) Schematic view of engineered deletion mutants. Each arc represents the deleted region in the mutant ET1 (dark blue), ET2 (green), ET3 (brown) and ET4 (grey). (B) Reaction norms of fitness for deletion mutants and wild type in 4 selective environments: M, S, MS, M/S, and each half-environment of M/S (M→S and S→M). (C) Transition time from S to M. (D) Fitness cost at stationary phase estimated as the fitness drop from hour 28 to hour 48. (E–G) Succinate-grown cultures with the following treatments: E, ampicillin (12.5 μg/mL); F, arsenate (30 mM); G, 36°C. Relative growth rate or final OD_{600} (optical density) was calculated as the ratio of with and without treatment. Error bars represent 95% confidence intervals and significant differences from wild-type are indicated by *($P<0.05$).
doi:10.1371/journal.pgen.1002651.g002

may account for the surprisingly high frequencies of DT1 in methanol and low frequency in methanol/succinate switching environments. Given that the various deletions appeared (above the limit of detection) in the second half of this 1500 generation experiment, other mutations would have already been present that may alter the selective effect of these losses (Text S1).

Although the large-scale deletions from the megaplasmid of *M. extorquens* AM1 were beneficial in the laboratory environment, further tradeoffs suggest that loss of this region would have consequences in natural environments. Unlike regular plasmids, megaplasmids and minichromosomes (or 'chromids') are long-term replicons residing in more than 10% of bacterial genomes across markedly different life styles [27]. The GC%, coding density and the percentage of repeat region of the megaplasmid in AM1 are compatible with the main chromosome but very different from the other 3 small plasmids present in this genome, indicating its long-term existence in this strain. We first examined the potential functions of the megaplasmid by COG analysis, which showed an overrepresentation of genes related to metabolic functions in deleted regions (X^2 test, $P<0.0001$, Figure S4). This is consistent with the observation of other reduced genomes [7]. Furthermore, the predicted functions of the genes encoded within the deleted regions were consistent with a lack of essentiality due to duplicate copies of potentially essential genes on the main chromosome. Indeed, with a fairly liberal definition of homology (minLrap≥0.8; maxLrap≥0; identity≥60%) there are 159 genes on the megaplasmid that have the homologs on the main chromosome. As 113 of these are found in DT1, a significant overrepresentation relative to the rest of the megaplasmid (X^2 test, $P<0.0001$), and all regions with synteny with the chromosome for ten or more genes are located in the deleted region, some of the benefit may have come from removing these possible redundancies. On the other hand, many genes putatively involved in stress responses would have been lost (Table S5). We therefore tested the deletion types across a panel of stresses, revealing that ET1 and ET4 had decreased resistance to ampicillin and arsenate (Figure 2E and 2F), and increased growth at the upper end of the temperature range of *M. extorquens* AM1 (Figure 2G). The loss of two sigma factors (Figure S5) and genes shown to be involved in leaf surface colonization [28] by these deletions lends further support that some of these genes contributed to the ecology of this strain.

Conclusions

These data have provided a rare opportunity to demonstrate that selection for gene loss contributed to the repeated, large-scale removal of accessory functions from adapting genomes. The selection regime we applied was a seasonal environment of growth and starvation, but since only one or two supplied resources and all other environmental factors were held constant, this rendered many functions unnecessary. It is quite common for plasmids bearing antibiotic resistance genes or toxins to be lost when these functions go unrewarded; however, this process differs substantially what is described here in terms of the scale of genome change, the presence of genes that would be essential if it were not for a duplicate copy, as well as the mechanism of loss (unfaithful segregation vs. homologous recombination).

Given that so many genes were lost in these deletion events, future work will be required to pin down whether few or many genes contribute to the observed phenotypes and by how much. Numerous stress response genes were lost in these events, and it has been in multiple cases that there can be tradeoffs between growth capacity and stress response in environments ranging from chemostats [29] to long-term stationary phase [30]. Similarly, the deletions that sped growth on most substrates led to an impaired capacity to deal with nutrient switches, starvation, and the toxic effects of an antibiotic and a toxic metal. Although these large-scale losses were successful due to the benefit they conferred in the flask, it is quite likely that they would impart tradeoffs in components of the natural environment inhabited by *Methylobacterium*.

Selection-driven loss of accessory genes can rapidly limit the niche of a given lineage, resulting in restricted lifestyle and lowering both N_e and access to horizontal gene transfer with other members of the species. Indeed, aspects of our laboratory conditions and starting strain - a sudden restriction in niche breadth and now unnecessary accessory functions present in contiguous islands - commonly occurs in natural environments, such as the establishment of chronic infections by opportunistic pathogens where analogous deletion events have been identified [13–15]. Smaller, more isolated populations in which purifying selection for previously useful functions is absent can lead to further genome reductions as drift becomes increasingly relevant. Thus, although in other scenarios bottlenecks leading to loss of functions via drift could initiate specialization, our results emphasize the potential for selection-driven, large-scale deletions of unnecessary genes as a route towards a limited niche and the beginning of a path leading to further genome changes.

Materials and Methods

Experimental evolution populations

This paper examines isolates from 32 populations that were founded from two nearly isogenic strains of wild-type *Methylobacterium extorquens* AM1, CM501 and CM502, which have pink and white colony color, respectively [31]. These populations evolved in four different environments each with 8 replicates (odd numbers founded by CM501; even by CM502): methanol (M, 15 mM, 'A' populations), succinate (S, 3.5 mM, 'B' populations), a mixture (MS) of methanol (7.5 mM) and succinate (1.75 mM) ('C' populations), and alternating (M/S) between methanol (15 mM) and succinate (3.5 mM) ('D' populations). The general selective regime, minimal medium and culturing conditions utilized were described previously along with the initial examination of the dynamics of adaptation and specialization of the A and B populations [22]. The C and D populations were evolved in the same conditions except for the mixed or alternating substrate conditions. Briefly, populations were grown in 9.6 mL of medium and cultured at 30°C in 50 mL flasks with 225 rpm shaking. Serial transfers were performed every 48 hours using 1/64 dilutions (*i.e.*, 6 generations) with a population size at the end of each cycle of $\sim 2\times10^9$. Three or four evolved isolates were obtained from generation 1500 of each population with preference for different colony morphologies, where apparent. From each population, one or two isolate(s) were chosen to test in genomic microarray analysis, and the remaining colonies were screened for deletions via PCR (Table S1).

Mutation accumulation system

Ten mutation accumulation lines were founded by CM501 and prorogated at 30°C on solid media comprised of half nutrient agar and half 'hypho' agar containing succinate (7.5 mM final concentration) [31] to allow rapid colony formation. For each lineage, every 3.5 days the last colony on the streak line was picked as a random sample and streaked on a new plate. The population expanded from one cell to approximately 10^6 cells in a colony each passage, representing ~20 generations, and was repeated 75 times (~1,500 generations).

Deletion detection via comparative genomic hybridization (CGH)

DNA isolation was performed using the Wizard Genomic DNA Purification Kit (Promega, Madison, WI) following the manufacturer's protocol. Deletions in evolved strains were identified using comparative genomic hybridization arrays performed by MOgene Inc. (St. Louis, MO), a certified Agilent service provider. The custom arrays spotted with the ancestor genome were designed, printed, and probed as described [32]. Without the necessity to detect quantitative signals, each sample was labeled with either Cy3 or Cy5 and hybridized once with a sample labeled with the other dye. In total, 25 hybridizations were done for 45 samples (44 evolved strains and the ancestor), including three control experiments (Table S2).

Deletion confirmation by PCR and sequencing

To confirm each deletion, one primer outside (p1 & p4) and inside (p2 & p3) that region was designed for each side. The deletion was confirmed if fragment was amplified by p1 & p4 but no product was amplified by p1 & p2 or p3 & p4. For fragments shorter than 1 kb, exact junctions were verified via sequencing. Products longer than 1 kb were analyzed via restriction digests to compare with the predicted patterns from the genome sequence. All confirmed deletions were consistent with array results. The precise junctions of all deletions on the main chromosome were identified except two of the deletions in CM1055 and CM1820 due to the presence of multiple repeat elements around their flanking regions. For the deletions on the megaplasmid, we only focused on the parallel pattern of the deletions and did not confirm each various subtype with their slightly different endpoints.

For detecting deletions in isolates not screened via CGH, we designed 4 pairs of primers to amplify regions across DT1, each with upstream and downstream pairs (Table S3). We classified isolates into 4 major types based on the PCR results (DT1 with 2 subtypes): DT1a (negative results from all), DT1b (negative result from R1, R2, and R3 and positive result from R4), DT2 (negative result from R1&R2 and positive result from R3&R4), DT4 (positive result from R1&R2 and negative result from R3&R4; not found in any population), and no deletion (positive results from all). The deletion in CM1194 was categorized as DT3a based on the array data; the deletion in CM1182 was categorized as DT3b based on the negative result from R3 but positive results from the other 3.

Construction of deletion mutants

Allelic exchange plasmids for generating deletion mutants were constructed based on pCM433, a *sacB*-based suicide vector [31]. PCR products of regions upstream and downstream of each deletion were amplified and consecutively cloned into pCM433 to generate pML4, pML5, pML7 and pML9 (Table S4). In order to reduce false-positives, a second selection marker, *kan*, with *loxP* excision sites amplified from pCM184 [33] was introduced into each of the plasmids between the upstream and downstream regions to generate pML10, pML11, pML12 and pML13, respectively (Table S4). Each of these donor plasmids was then introduced into the wide type strain (CM501) via triparental conjugations as previously described [31]. Single-crossover recombinants were selected with tetracycline (Tet, 10 μg mL^{-1}) and then double-crossover recombinants were selected with kanamycin (Kan, 50 μg mL^{-1}) and sucrose (5% wt/vol.). For each deletion type, we saved three independent clones through the cloning steps. These were each confirmed by PCR to contain the correct deletion and all three were tested for a consistent phenotype. The *kan* marker was then excised by *cre* recombinase as before [33] to generate the desired unmarked deletion mutants (Table S1).

Growth and fitness assays

We performed the growth and fitness assays following a previously described procedure [22] with a few modifications. Briefly, three replicate cultures of each strain were inoculated and acclimated in minimal medium supplemented with carbon sources in 48-well plates (Corning, Lowell, MA) at 30°C, 650 rpm, 1 mm orbit and a total volume of 640 μL in each well. Growth curves were then obtained by following the change in OD_{600} (Victor^2 plate reader, Perkin Elmer, Waltham, MA). The transition time between growth phases observed during growth on MS (M:S = 7:1) was estimated as before [34]. Growth rates and regression lines for each phase were calculated (Phase I: $y = a_1+b_1x$; Phase II: $y = a_2+b_2x$), the OD_{600} at the time of transition (OD_t) was determined as the average of two OD_{600} values with the minimum change during the transition phase, and the effective transition time was obtained as the difference between the two time values (x_1, x_2) where the estimated regression lines were equal to OD_t.

Fitness of each strain was measured as before [22] by competing each evolved or constructed strain against a fluorescently labeled ancestor (CM1179) strain in 48-well plates with initial volumetric ratio of 1:1. Due to the small fitness changes for certain strains, competition assays were run for 4 cycles of growth (*i.e.*, 8 days). The ratio of non-fluorescent cells in mixed populations was measured by passing population samples before (R_0) and after 4 cycles of competition growth (R_4) through a BD LSR II flow cytometer (BD Biosciences, San Jose, CA). Fitness values (W) were calculated by following equation:

$$W = \ln\left(\frac{R_4 \cdot 64^4}{R_0}\right) \Big/ \ln\left(\frac{(1-R_4)\cdot 64^4}{1-R_0}\right)$$

To estimate the fitness cost on succinate during stationary phase, cultures were also sampled at hour 28 (early stationary phase), such that the fitness cost was estimated as the difference in fitness values calculated between hours 0 to 28 vs. 0 to 48 (using 9 replicates per strain).

General stress response assays

Disc diffusion assays were done to test for sensitivity on formaldehyde, SDS, peroxide, a trace metal mix, salt, arsenate and amplicillin. Bacteria were grown to stationary phase (OD_{600}~1.5) in regular hypho medium supplied with 3× succinate (10.5 mM) . Five mL of this culture was mixed with 60 mL of 42°C pre-warmed soft agar (0.75%, with 15 mM succinate), and 5 mL of this mixture was poured onto hypho agar plates with 15 mM succinate. Disks were placed at the center of the plates and aliquots (5 μL) of formaldehyde (37%), SDS (10%), peroxide (30%), a trace metal mix (1000×) (Delaney et al. unpublished), NaCl (1 M), sodium arsenate (10% w/v) or amplicillin (100 mg/mL) were added on the filter discs. Diameters of growth inhibition were measured after 4 days.

Exponential-phase cells growing on succinate (OD_{600}~0.5) were used in heat shock and UV resistance assays. Cells were transferred to 55°C for 15 min for heat shock or exposed to 312 nm UV light for 15 min for UV resistance assays. Suspensions were then diluted and plated onto hypho agar containing 15 mM succinate, and colonies were counted after 4 days of 30°C incubation.

Additionally, succinate-grown cultures were tested in liquid medium with the following treatments: formaldehyde (1–5 mM), SDS (10^{-1}–10^{-5}‰), peroxide (10^{-1}–10^{-5}‰), trace metal mix (2–20×), salt (5–500 mM), ampicillin (12.5–50 μg/mL), sodium arsenate (20–50 mM), UV exposure prior to growth (1–20 min), or heat stress during growth (32–36°C). Final OD_{600} or relative growth rates were calculated as the ratio of treatment to control.

Supporting Information

Figure S1 Average fitness increase of evolved populations in their selective environments. The boxplot shows the mean and variation of 25 isolates in each environment. Average fitness increases are 14.5%, 26.0%, 20.7%, 24.8% for A (M), B (S), C (MS) and D (M/S) populations, respectively. As reported previously [22], a couple of these strains were actually less fit than the ancestor, which likely represent genotypes that exist due to frequency-dependent interactions such as cross-feeding.
(TIF)

Figure S2 Relative growth rates and additive effects in fitness values of ET2 and ET4 in various environments. Dots represent the relative growth rates of mutants in all 5 environments, calculated as the ratio to the wild-type. Error bars represent 95% confidence intervals. Similar patterns were found as in fitness values except in S→M and M→S where the fitness of ET1 and ET4 change significantly but the growth rates remain the same, when compared to the corresponding environment (M and S, respectively). The light blue dash line represents the product of fitness values for ET2 and ET4, which is not significantly different from the fitness values of ET1 in all environments. The result indicates 'non-epistatic' interaction between ET2 and ET4; the proportional effect of ET2 and ET4 is unchanged when present together in ET1.
(TIF)

Figure S3 Viable counts of selected deletion mutants in 4 environments (M, S, M→S, S→M). All mutants and wild type have similar viable counts even after 96 hours. Less than 15% drop of viable counts was observed for all mutants.
(TIF)

Figure S4 Functional analysis of DT1 versus undeleted region on the megaplsmid. The number of ORFs for each major functional category was calculated based on COG classification. There are substantially more metabolic related genes in DT1 region than the undeleted region.
(TIF)

Figure S5 Phylogeny of sigma factors in *M. extorquens* AM1 (META1, pink text; META2, orange text) and closely related strains: *M. extorquens* DM4 (METDI), CM4 (Mchl), PA1 (Mext), *M. populi* BJ001 (Mpop). Five groups of sigma factors are colored based on the annotation. Arrows indicate the sigma factors which locate in the region of ET2 (green) and ET4 (grey). META2_0154 (ECF type) and META2_0121 (sigma 24) are conserved in all *M. extorquens* strains, suggesting a potential function of those two sigma factors.
(TIF)

Table S1 *Methylobacterium* strains used in the study.
(DOCX)

Table S2 Deletions detected by CGH arrays.
(DOCX)

Table S3 Primer list.
(DOCX)

Table S4 Plasmid list.
(DOCX)

Table S5 Functional gene list within deletion region.
(DOCX)

Text S1
(DOCX)

Acknowledgments

We thank members of the Marx lab, Colleen Cavanaugh, Vanja Klepac-Ceraj, and Chin-Horng Kuo for discussions and comments on the manuscript and Shaukat Rangwala for exemplary service while handling our CGH arrays.

Author Contributions

Conceived and designed the experiments: M-CL CJM. Performed the experiments: M-CL CJM. Analyzed the data: M-CL CJM. Contributed reagents/materials/analysis tools: M-CL CJM. Wrote the paper: M-CL CJM.

References

1. Kuo C, Moran NA, Ochman H (2009) The consequences of genetic drift for bacterial genome complexity. Genome Res 19: 1450–1454.
2. Lynch M (2006) Streamlining and simplification of microbial genome architecture. Annu Rev Microbiol 60: 327–349.
3. Lawrence JG, Ochman H (1998) Molecular archaeology of the *Escherichia coli* genome. Proc Natl Acad Sci USA 95: 9413–9417.
4. Welch RA, Burland V, Plunkett G, Redford P, Roesch P, et al. (2002) Extensive mosaic structure revealed by the complete genome sequence of uropathogenic *Escherichia coli*. Proc Natl Acad Sci USA 99: 17020–17024.
5. Lan R, Reeves PR (2000) Intraspecies variation in bacterial genomes: the need for a species genome concept. Trends Microbiol 8: 396–401.
6. Moran NA, Mira A (2001) The process of genome shrinkage in the obligate symbiont *Buchnera aphidicola*. Genome Biol 2: research0054.
7. Moran NA (2002) Microbial minimalism: Genome reduction in bacterial pathogens. Cell 108: 583–586.
8. Ochman H, Moran NA (2001) Genes lost and genes found: evolution of bacterial pathogenesis and symbiosis. Science 292: 1096–1099.
9. McCutcheon JP, Moran NA (2011) Extreme genome reduction in symbiotic bacteria. Nat Rev Microbiol 10: 13–26.
10. Dufresne A, Garczarek L, Partensky F (2005) Accelerated evolution associated with genome reduction in a free-living prokaryote. Genome Biol 6: R14.
11. Giovannoni SJ, Tripp HJ, Givan S, Podar M, Vergin KL, et al. (2005) Genome streamlining in a cosmopolitan oceanic bacterium. Science 309: 1242–1245.
12. Frost LS, Leplae R, Summers AO, Toussaint A (2005) Mobile genetic elements: the agents of open source evolution. Nat Rev Microbiol 3: 722–732.
13. Cramer N, Klockgether J, Wrasman K, Schmidt M, Davenport CF, et al. (2011) Microevolution of the major common *Pseudomonas aeruginosa* clones C and PA14 in cystic fibrosis lungs. Environ Microbiol 13: 1690–1704.
14. Ernst RK, D'Argenio DA, Ichikawa JK, Bangera MG, Selgrade S, et al. (2003) Genome mosaicism is conserved but not unique in *Pseudomonas aeruginosa* isolates from the airways of young children with cystic fibrosis. Environ Microbiol 5: 1341–1349.
15. Smith EE, Buckley DG, Wu Z, Saenphimmachak C, Hoffman LR, et al. (2006) Genetic adaptation by *Pseudomonas aeruginosa* to the airways of cystic fibrosis patients. Proc Natl Acad Sci USA 103: 8487–8492.
16. Maurelli AT, Fernández RE, Bloch CA, Rode CK, Fasano A (1998) "Black holes" and bacterial pathogenicity: a large genomic deletion that enhances the virulence of *Shigella spp.* and enteroinvasive *Escherichia coli*. Proc Natl Acad Sci USA 95: 3943–3948.
17. Nilsson A, Koskiniemi S, Eriksson S, Kugelberg E, Hinton J, et al. (2005) Bacterial genome size reduction by experimental evolution. Proc Natl Acad Sci USA 102: 12112–12116.

18. Barrick JE, Yu DS, Yoon SH, Jeong H, Oh TK, et al. (2009) Genome evolution and adaptation in a long-term experiment with *Escherichia coli*. Nature 461: 1243–1247.
19. Zhong S, Khodursky A, Dykhuizen DE, Dean AM (2004) Evolutionary genomics of ecological specialization. Proc Natl Acad Sci USA 101: 11719–11724.
20. Cooper VS, Schneider D, Blot M, Lenski RE (2001) Mechanisms causing rapid and parallel losses of ribose catabolism in evolving populations of *Escherichia coli* B. J Bacteriol 183: 2834–2841.
21. Delmotte N, Knief C, Chaffron S, Innerebner G, Roschitzki B, et al. (2009) Community proteogenomics reveals insights into the physiology of phyllosphere bacteria. Proc Natl Acad Sci USA 106: 16428–16433.
22. Lee M-C, Chou H-H, Marx CJ (2009) Asymmetric, bimodal trade-offs during adaptation of *Methylobacterium* to distinct growth substrates. Evolution 63: 2816–2830.
23. Vuilleumier S, Chistoserdova L, Lee M-C, Bringel F, Lajus A, et al. (2009) *Methylobacterium* genome sequences: a reference blueprint to investigate microbial metabolism of c1 compounds from natural and industrial sources. PLoS ONE 4: e5584.
24. Chou H-H, Chiu H-C, Delaney NF, Segrè D, Marx CJ (2011) Diminishing returns epistasis among beneficial mutations decelerates adaptation. Science 332: 1190–1192.
25. Moran NA, McLaughlin HJ, Sorek R (2009) The dynamics and time scale of ongoing genomic erosion in symbiotic bacteria. Science 323: 379–382.
26. Novichkov PS, Wolf YI, Dubchak I, Koonin EV (2009) Trends in prokaryotic evolution revealed by comparison of closely related bacterial and archaeal genomes. J Bacteriol 191: 65–73.
27. Harrison PW, Lower RPJ, Kim NKD, Young JPW (2010) Introducing the bacterial 'chromid': not a chromosome, not a plasmid. Trends Microbiol 18: 141–148.
28. Gourion B, Rossignol M, Vorholt JA (2006) A proteomic study of *Methylobacterium extorquens* reveals a response regulator essential for epiphytic growth. Proc Natl Acad Sci USA 103: 13186–13191.
29. Notley-McRobb L, King T, Ferenci T (2002) rpoS mutations and loss of general stress resistance in Escherichia coli populations as a consequence of conflict between competing stress responses. J Bacteriol 184: 806–811.
30. Finkel SE (2006) Long-term survival during stationary phase: evolution and the GASP phenotype. Nat Rev Microbiol 4: 113–120.
31. Marx C (2008) Development of a broad-host-range *sacB*-based vector for unmarked allelic exchange. BMC Res Notes 1: 1.
32. Okubo Y, Skovran E, Guo X, Sivam D, Lidstrom ME (2007) Implementation of microarrays for *Methylobacterium extorquens* AM1. Omics 11: 325–340.
33. Marx CJ, Lidstrom ME (2002) Broad-host-range *cre-lox* system for antibiotic marker recycling in gram-negative bacteria. Biotechniques 33: 1062–1067.
34. Vasi F, Travisano M, Lenski RE (1994) Long-term experimental evolution in *Escherichia coli*. II. Changes in life-history traits during adaptation to a seasonal environment. Am Nat 144: 432–456.

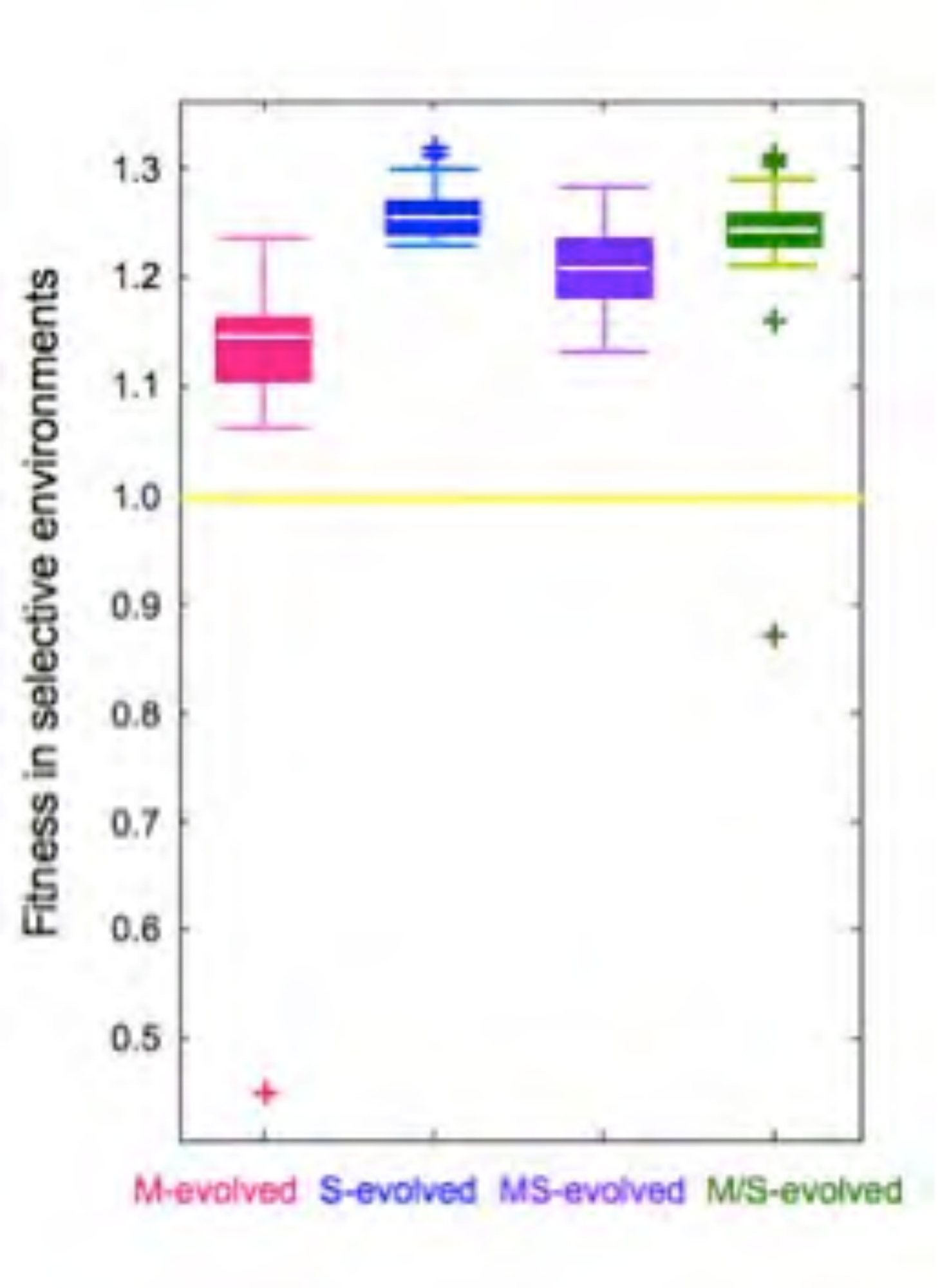
Fitness in selective environments
1.3
1.2
1.1
1.0
0.9
0.8
0.7
0.6
0.5
M-evolved
S-evolved
MS-evolved
M/S-evolved

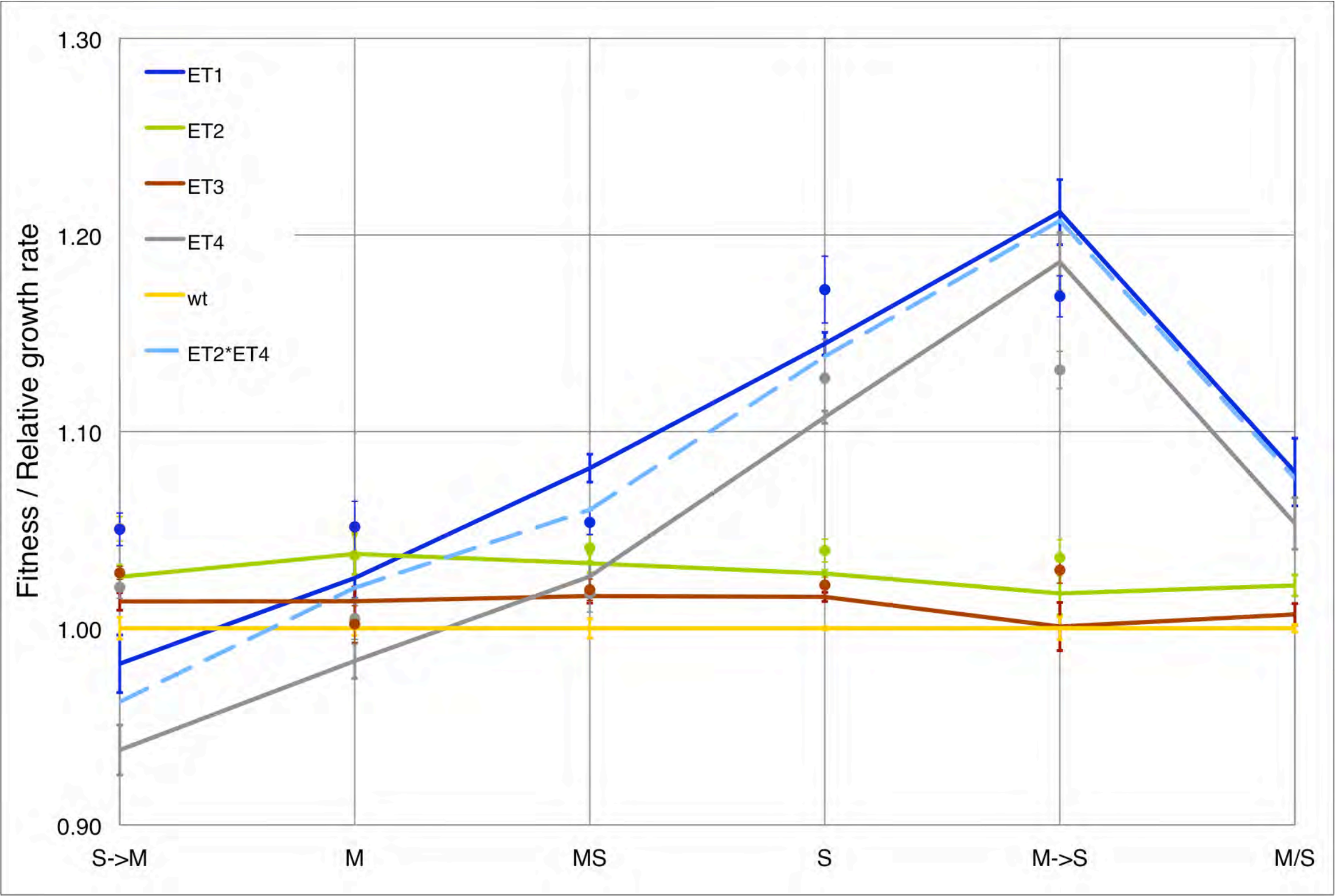
1.30
1.20
1.10
1.00
0.90
Fitness / Relative growth rate
ET1
ET2
ET3
ET4
wt
ET2*ET4
S->M
M
MS
S
M->S
M/S

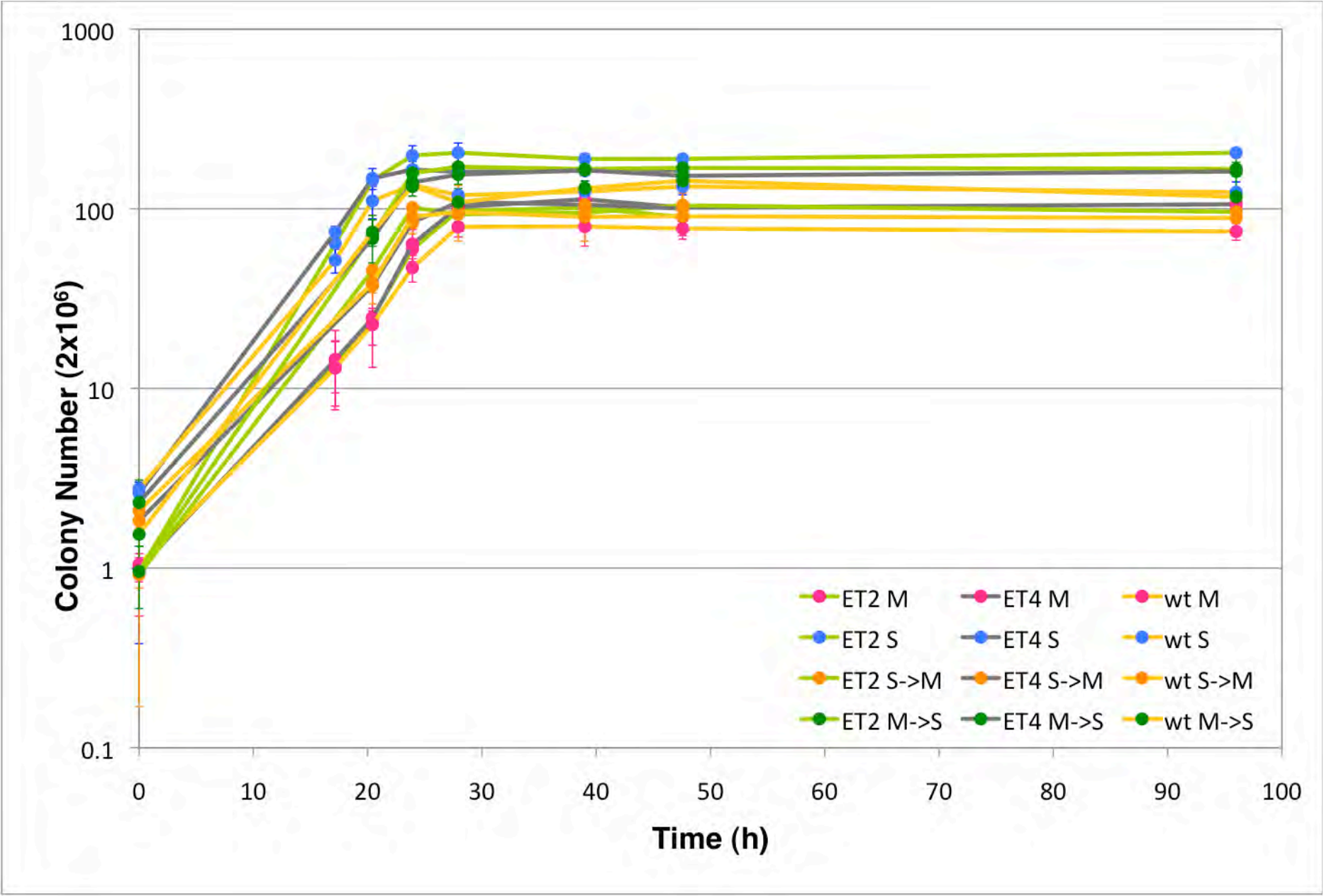
1000
100
10
1
0.1
Colony Number (2x10⁶)
0
10
20
30
40
50
60
70
80
90
100
Time (h)
ET2 M
ET4 M
wt M
ET2 S
ET4 S
wt S
ET2 S->M
ET4 S->M
wt S->M
ET2 M->S
ET4 M->S
wt M->S

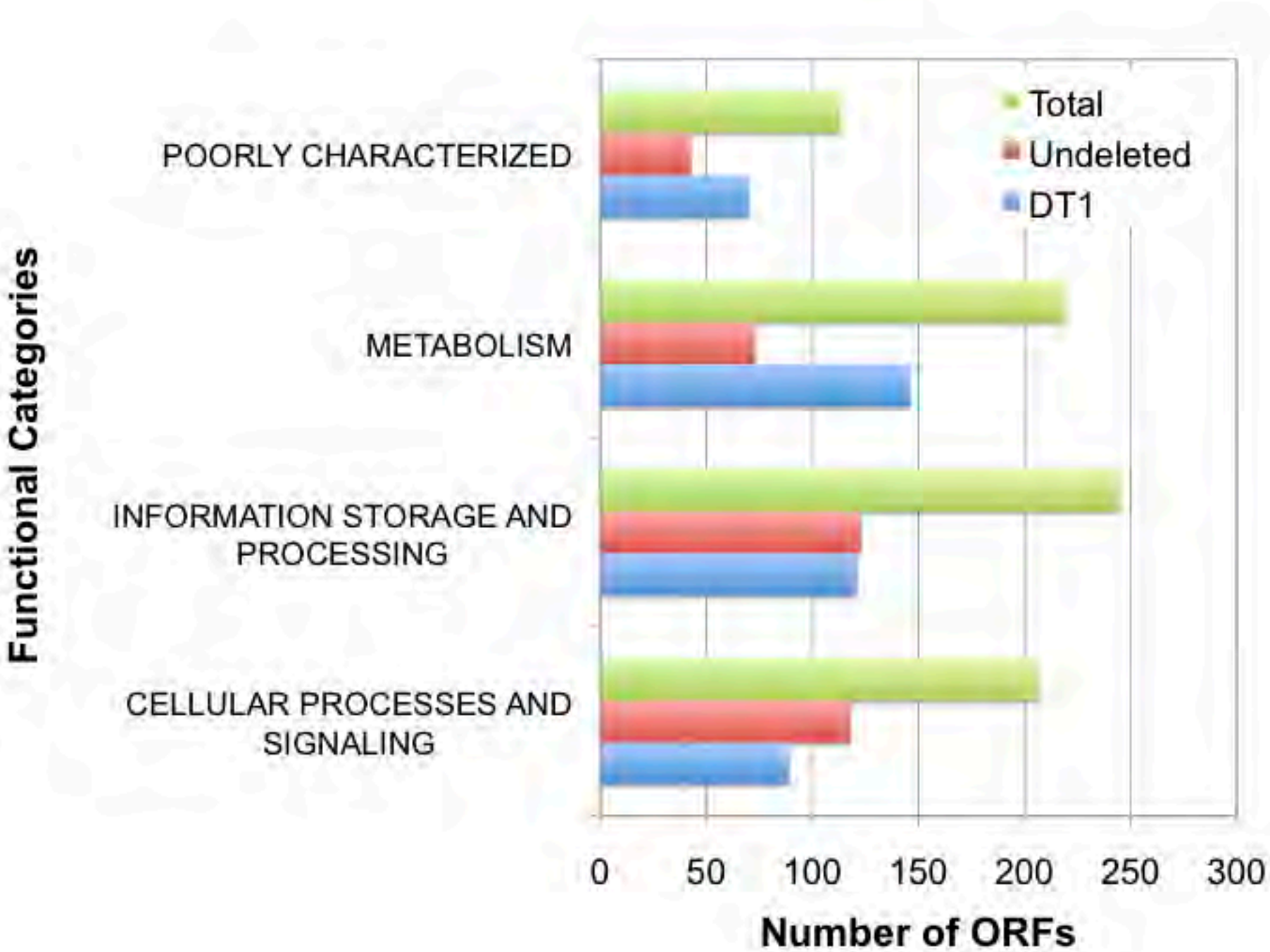
Total
Undeleted
DT1
POORLY CHARACTERIZED
METABOLISM
INFORMATION STORAGE AND PROCESSING
CELLULAR PROCESSES AND SIGNALING
Functional Categories
0
50
100
150
200
250
300
Number of ORFs

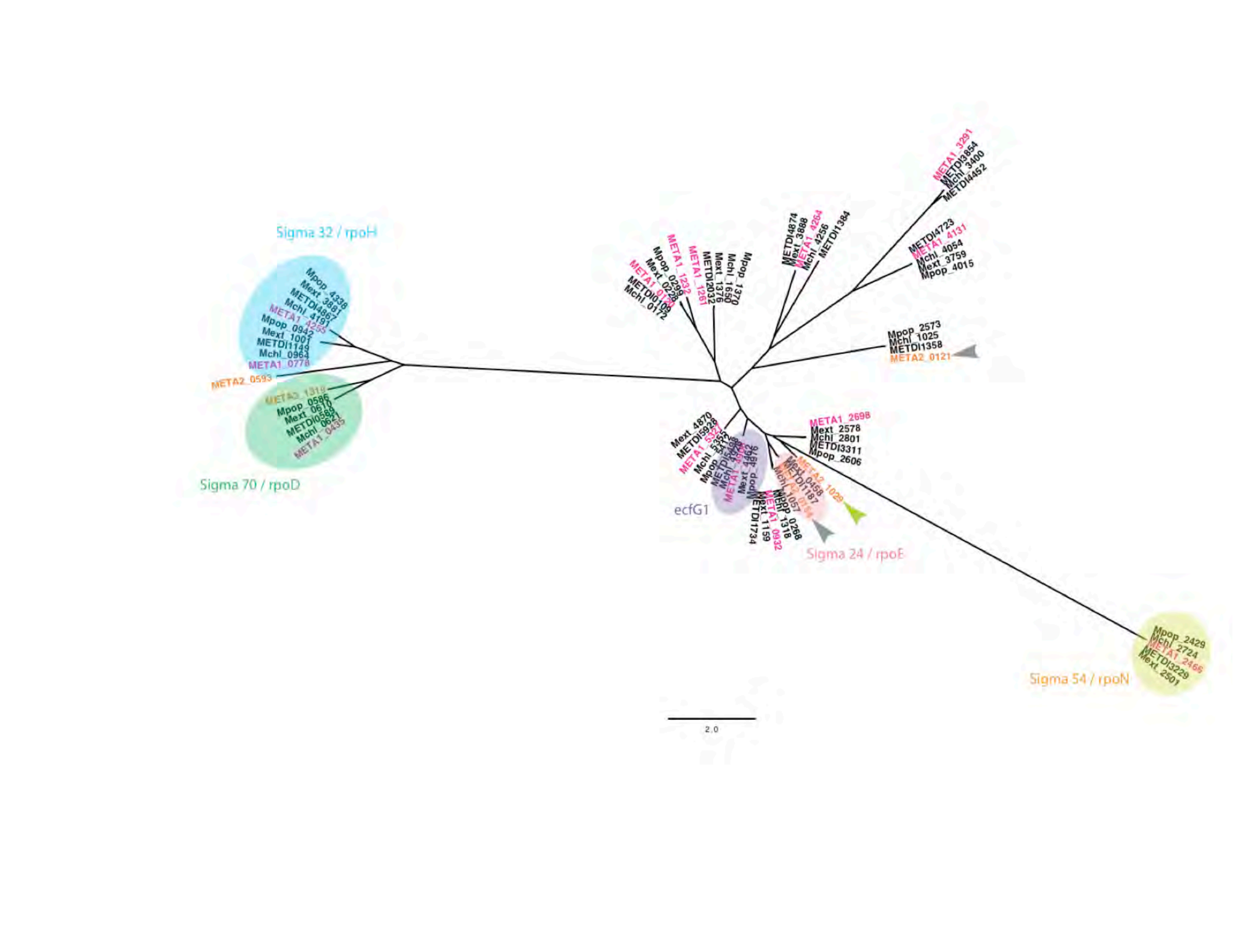
Sigma 32 / rpoH
Mpop_4338
Mext_3891
METDI4867
Mchl_4191
META1_4295
Mpop_0942
Mext_1001
METDI1149
Mchl_0964
META1_0778
META2_0593
META3_1319
Mpop_0586
Mext_0610
METDI0589
Mchl_0621
META1_0435
Sigma 70 / rpoD
META1_1232
Mpop_0298
Mext_0298
METDI0298
Mchl_0172
META1_1281
Mext_1376
METDI2032
Mpop_1370
Mchl_1650
METDI4874
Mext_3888
META1_4264
Mchl_4256
METDI1384
METDI4723
META1_4131
Mchl_4054
Mext_3759
Mpop_4015
METDI3854
Mchl_3400
METDI4452
Mpop_2573
Mchl_1025
METDI1358
META2_0121
Mext_4870
METDI5928
META1_5321
Mchl_5325
Mpop_5175
Mext_4962
Mpop_4976
ecfG1
META1_2698
Mext_2578
Mchl_2801
METDI3311
Mpop_2606
META2_1029
Mext_0458
METDI1187
Mchl_1057
Mpop_0268
Mext_1159
METDI1734
META1_0932
Sigma 24 / rpoE
Mpop_2429
Mchl_2724
META1_2466
METDI3229
Mext_2501
Sigma 54 / rpoN
2.0

Table S1. *Methylobacterium* strains used in the study

Strain	Source	Colony Morphology	Hybridization pair	Deletion region Chromosome (META1)	Deletion region Megaplasmid (META2)	Big deletion type determined by PCR[※]
CM501	Ancestor	Pink	3,4,25	None	None	--
CM502	Ancestor	White	--	None	None	--
CM1203	CM501, Δ*hprA*	Pink	1	None	None	--
CM1027	A1	Pink, Large	--	--	--	DT1a
CM1028	A1	Pink, Medium	13	3908875~3921127 *	822917~844898 881288~206285[†]	DT1a
CM1029	A1	Pink, Small	--	--	--	DT1a
CM1030	A2	White, Large	21	ND	881288~206285[†]	DT1a
CM1031	A2	White, Medium	--	--	--	DT1a
CM1032	A2	White, Small	14	ND	838627~211269	DT1a
CM1033	A3	Pink, Large	--	--	--	DT1a
CM1034	A3	Pink, Medium	15	3894244~3955912 *	ND	ND
CM1035	A3	Pink, Small	--	--	--	ND
CM1036	A4	White, Large	16	ND	857393~168962	DT1b
CM1037	A4	White, Medium	--	--	--	DT1b
CM1038	A4	White, Small	--	--	--	DT1b
CM1039	A5	Pink, Large	--	--	--	ND
CM1040	A5	Pink, Small	--	--	--	ND
CM1041	A5	Pink, Dark pink	22	ND	855329~211852[†]	DT1a
CM1042	A5	Pink, Pale pink	17	ND	ND	ND
CM1043	A6	White, Large	18	ND	881288~206285[†]	DT1a
CM1044	A6	White, Medium	2	ND	281915~306778* 881288~206285[†]	DT1a
CM1045	A6	White, Small	--	--	--	DT1a
CM1046	A7	Pink, Large	19	ND	ND	ND
CM1047	A7	Pink, Medium	--	--	--	DT1a
CM1048	A7	Pink, Small	--	--	--	DT1a
CM1049	A8	White, Large	--	--	--	ND
CM1050	A8	White, Medium	20	ND	826162~205962	DT1a
CM1051	A8	White, Small	--	--	--	DT1a
CM1086	B1	Pink, Large	--	--	--	DT1a
CM1087	B1	Pink, Small	13	3894244~3955912 *	881288~206285[†]	DT1a
CM1088	B1	Pink, Pale pink	--	--	--	DT1a
CM1089	B2	White, Large	--	--	--	DT1a
CM1090	B2	White, Medium	14	ND	881288~206285[†]	DT1a
CM1091	B2	White, Small	--	--	--	DT1a
CM1092	B3	Pink, Large	--	--	--	DT1a
CM1093	B3	Pink, Medium	--	--	--	DT1a
CM1094	B3	Pink, Small	15	ND	881288~206285[†]	DT1a
CM1095	B4	White, Large	16	4133302~4147632 *	855329~211852[†]	DT1a
CM1096	B4	White, Medium	--	--	--	DT1a
CM1097	B4	White, Small	2	4133302~4147632 * 3894244~3955912 *	855329~211852[†]	DT1a
CM1098	B5	Pink, Small	17	4133303~4155430 *	855329~211852[†]	DT1a
CM1099	B5	Pink, Dark pink	21	3894244~3955912	855329~211852[†]	DT1a

				4133303~4155430*		
CM1100	B5	Pink, Pale pink	--	--	--	DT1a
CM1104	B6	White, Large	22	ND	881288~206285†	DT1a
CM1105	B6	White, Medium	18	ND	881288~206285†	DT1a
CM1106	B6	White, Small	--	--	--	DT1a
CM1107	B6	White, Small	--	--	--	DT1a
CM1101	B7	Pink, Large	--	--	--	DT2
CM1102	B7	Pink, Medium	--	--	--	DT2
CM1103	B7	Pink, Small	19	ND	883700~70551	DT1b
CM1108	B8	White, Large	--	--	--	DT1b
CM1109	B8	White, Medium	20	ND	855329~211852†	DT1a
CM1110	B8	White, Small	--	--	--	DT1a
CM1052	C1	Pink, Large	--	--	--	DT2
CM1053	C1	Pink, Medium	23	ND	883700~1150049	DT2
CM1054	C1	Pink, Small	3,5	2877651~2907157† 3894244~3955912*	881288~206285†	DT1a
CM1055	C2	White, Large	6	63646~80725	881288~206285†	DT1a
CM1056	C2	White, Large	--	--	--	DT1a
CM1057	C2	White, Small	--	--	--	DT1a
CM1058	C2	White, Small	--	--	--	DT1a
CM1059	C3	Pink, Large	--	--	--	DT1a
CM1060	C3	Pink, Medium	7	ND	881288~206285†	DT1a
CM1061	C3	Pink, Small	--	--	--	DT1a
CM1062	C4	White, Large	24	ND	881288~206285†	DT1a
CM1063	C4	White, Medium	8	ND	881288~206285†	DT1a
CM1064	C4	White, Small	--	--	--	DT1a
CM1065	C5	Pink, Small	--	--	--	DT1a
CM1066	C5	Pink, Dark pink	9	ND	881288~206285†	DT1a
CM1067	C5	Pink, Pale pink	--	--	--	DT1a
CM1068	C6	White, Large	10	3894244~3955912*	881288~206285†	DT1a
CM1069	C6	White, Medium	--	--	--	DT1a
CM1070	C6	White, Small	--	--	--	DT1a
CM1071	C7	Pink, Large	--	--	--	DT1a
CM1072	C7	Pink, Medium	11	4133299~4160613*	881288~206285†	DT1a
CM1073	C7	Pink, Small	25	ND	881288~206285†	DT1a
CM1074	C8	White, Large	12	3894244~3955912*	826162~205962	DT1a
CM1075	C8	White, Medium	--	--	--	DT1a
CM1076	C8	White, Small	--	--	--	DT1a
CM1181	D1	Pink, Large	4,5	ND	ND	ND
CM1182	D1	Pink, Medium	--	--	--	DT3b
CM1183	D1	Pink, Small	--	--	--	DT2
CM1184	D2	White, Large	--	--	--	DT2
CM1185	D2	White, Large	--	--	--	DT2
CM1186	D2	White, Small	6	ND	303859~318885 838627~1150049	DT2
CM1187	D3	Pink, Large	--	--	--	DT1b
CM1188	D3	Pink, Medium	7	ND	ND	ND
CM1189	D3	Pink, Small	1	ND	ND	ND
CM1190	D4	White, Large	--	--	--	DT2

CM1191	D4	White, Medium	8	ND	868402~22943	DT1b
CM1192	D4	White, Small	--	--	--	DT1b
CM1193	D5	Pink, Small	9	ND	857393~1150049	DT2
CM1194	D5	Pink, Dark pink	23	ND	1118314~1141380	DT3a
CM1195	D5	Pink, Pale pink	--	--	--	DT2
CM1820	D6	White, Large	24	476704~485541	838627~142461	DT1b
CM1821	D6	White, Medium	--	--	--	DT1b
CM1822	D6	White, Small	--	--	--	DT1a
CM1196	D7	Pink, Large	--	--	--	ND
CM1197	D7	Pink, Large	11	ND	ND	ND
CM1198	D7	Pink, Small	--	--	--	ND
CM1199	D7	Pink, Small	--	--	--	ND
CM1200	D8	White, Large	12	ND	883700~1150049	DT2
CM1201	D8	White, Medium	--	--	--	ND
CM1202	D8	White, Small	10	ND	ND	ND
CM2074	ET1 mutant of CM501	pink	--	None	878552~210322	ET1
CM2075	ET1 mutant of CM501	pink	--	None	878552~210322	ET1
CM2076	ET1 mutant of CM501	pink	--	None	878552~210322	ET1
CM2077	ET2 mutant of CM501	pink	--	None	878552~1159793	ET2
CM2078	ET2 mutant of CM501	pink	--	None	878552~1159793	ET2
CM2079	ET2 mutant of CM501	pink	--	None	878552~1159793	ET2
CM2080	ET4 mutant of CM501	pink	--	None	1161223~210322	ET4
CM2081	ET4 mutant of CM501	pink	--	None	1161223~210322	ET4
CM2082	ET4 mutant of CM501	pink	--	None	1161223~210322	ET4
CM2083	ET3 mutant of CM501	pink	--	None	1112224~1159793	ET3
CM2084	ET3 mutant of CM501	pink	--	None	1112224~1159793	ET3
CM2085	ET3 mutant of CM501	pink	--	None	1112224~1159793	ET3

* Deletion region was confirmed by PCR followed by sequence

† Deletion region was confirmed by PCR followed by restriction digestion

※ Deletion type was determined by four pairs of primers to amplify fragments: R1, R2, R3, R4 (see Table S3 for specific primer locations). DT1a: all 4 pairs gave negative results. DT1b: R1, R2, and R3 came back negative but R4 was positive. DT2: R1 and R2 came back negative but R3 and R4 were positive. DT3a: only one isolate has this deletion, which was detected by array. DT3b: R1, R2 and R4 came back positive but R3 was negative.

Table S2. Deletions detected by CGH arrays

Replicon	Region	Length	Strain	Adjacent IS[†]
META1	63646~80725	17079	CM1055	※
META1	476704~485541	8837	CM1820	※
META1	2877651~2907157	29506	CM1054	ISMex15*2
META1	3894244~3955912	61668	CM1034, CM1087, CM1054, CM1068, CM1074, CM1099	Repeat*2
META1	3908875~3921127	12252	CM1028	ISMex16*0
META1	4133302~4147632	14330	CM1095[§B4], CM1097[§B4]	ISMex4*1
META1	4133303~4155430	22127	CM1098[§B5], CM1099[§B5]	ISMex4*1
META1	4133299~4160613	27314	CM1072	ISMex4*1
META2	281915~306778	24863	CM1044	ISMex16*0
META2	303859~318885	15026	CM1186	ISMex8*2
META2	826162~205962	641260	CM1050, CM1074	ISMex9*2
META2	838627~1150049	311422	CM1186	ISMex5/ISMex10 *2
META2	838627~142461	565294	CM1820	ISMex5/ISMex10 *1
META2	838627~211269	634102	CM1032	ISMex5*2
META2	822917~844898	21981	CM1028	ISMex9*1
META2	855329~211852	617983	CM1041, CM1095[§B4], CM1097[§B4], CM1098[§B5], CM1099[§B5], CM1109	ISMex5*2
META2	857393~1150049	292656	CM1193	ISMex5*1
META2	857393~168962	573029	CM1036	ISMex5*1
META2	868402~22943	416001	CM1191	※
META2	881288~206285	586457	CM1028, CM1030, CM1043[§A6], CM1044[§A6], CM1054, CM1055, CM1060, CM1062[§C4], CM1063[§C4], CM1066, CM1068, CM1072[§C7], CM1073[§C7], CM1087, CM1090, CM1094, CM1104[§B6], CM1105[§B6]	ISMex3*2
META2	883700~1150049	266349	CM1053, CM1200	ISMex3*1
META2	883700~70551	448311	CM1103	ISMex3*1
META2	1118314~1141380	23068	CM1194	※

[†] Numbers after * represent the IS copy number in the ancestral genome. Ex: ISMex16*0 means the deletion was mediated by two newly inserted ISMex16.

※ No IS was found around the deletion but we have not ruled out the possibility that the deletion is mediated by newly inserted IS elements.

§ Identical deletions detected in isolates from the same population were counted as single event. In total, 46 deletion events were detected. Letters after § indicate the population number.

Table S3. Primer list

	Primer	Sequence	Replicon	Position		Length
R1	R1-f	CTT CGT CGA TTC AGC TCG TAC GT	META2	884409	884431	
	R1-r	CCT GCA ACC AAG TCC TCT ACC ATC	META2	884817	884840	431
R2	R2-f	GGG TGC TTG GCA ATG TCT TAG GAA	META2	1115938	1115961	
	R2-r	TTT CTT GCG TCT GTG CGA GCT TG	META2	1116295	1116317	379
R3	R3-f	TAA GCT TTC GCC TAA ACG CCT TCG	META2	1155765	1155788	
	R3-r	ATT CAC CGA GAC TGT CCC AGA AGA	META2	1156189	1156212	447
R4	R4-f	ACA TTC GGT GGC AAC TCC TGA AG	META2	205547	205569	
	R4-r	CCA CTG CGA CCG ATC TCT TAG TTC AT	META2	205965	205990	443
PC	PC-f	CAG CTC GAC CAG CTT ATC GTT G	META1	4653445	4653466	
	PC-r	ATC GTC TCC AAG TGC GGT G	META1	4654012	4653994	549

Table S4. Plasmid list

Plasmid	Description
pCM184	Broad-host range cre-lox allelic exch, *Amp^R, Kan^R, Tet^R
pCM433	Broad-host-range *sacB*-based allelic exchange vector, Amp^R, Chl^R, Tet^R
pML3	pCM433 with META2_877176~878552, Amp^R, Chl^R, Tet^R
pML4	pML3 with META2_210322~211783, Amp^R, Chl^R, Tet^R
pML5	pML3 with META2_1159793~1161223, Amp^R, Chl^R, Tet^R
pML6	pCM433 with META2_210322~211783, Amp^R, Chl^R, Tet^R
pML7	pML6 with META2_1159793~1161223, Amp^R, Chl^R, Tet^R
pML8	pCM433 with META2_1110807~1112224, Amp^R, Chl^R, Tet^R
pML9	pML8 with META2_1159793~1161223, Amp^R, Chl^R, Tet^R
pML10	pML4 with *loxP-Kan-loxP*, Amp^R, Chl^R, Tet^R, Kan^R
pML11	pML5 with *loxP-Kan-loxP*, Amp^R, Chl^R, Tet^R, Kan^R
pML12	pML7 with *loxP-Kan-loxP*, Amp^R, Chl^R, Tet^R, Kan^R
pML13	pML9 with *loxP-Kan-loxP*, Amp^R, Chl^R, Tet^R, Kan^R

* Amp (ampicillin), Chl (chloramphenicol), Kan (kanamycin), Tet (tetracycline)

Table S5. Functional gene list within deletion region*

Gene ID	Begin	End	Length	Gene	Product
META2_0021	34645	37704	3060	*nrd*	Ribonucleoside-diphosphate reductase
META2_0052	62867	64453	1587		Beta-lactamase family protein
META2_0064	72260	72817	558		Signal receiver domain protein
META2_0084	89378	92524	3147		Heavy metal efflux pump, CzcA family
META2_0101	104280	105572	1293		Conserved hypothetical protein, putative Type II site-specific deoxyribonuclease
META2_0113	112567	115731	3165		Heavy metal efflux pump, CzcA family
META2_0121	120692	121300	609		RNA polymerase ECF-type sigma factor
META2_0140	134208	135620	1413	*pyk*	Pyruvate kinase
META2_0142	136331	137077	747	*arsH*	Arsenate resistance protein ArsH
META2_0143	137128	137487	360	*arsR2*	Transcriptional regulator, ArsR family, ArsR2
META2_0144	137480	138007	528	*arsC3*	Arsenate reductase
META2_0145	138007	138432	426	*arsC*	Arsenate reductase
META2_0147	138708	139508	801		Arsenite efflux pump ACR3 (fragment)
META2_0150	141288	143048	1761		Peptidase S8 and S53, subtilisin, kexin, sedolisin precursor
META2_0154	143577	144257	681		RNA polymerase sigma-24 subunit, ECF subfamily
META2_0155	144738	146327	1590		Filamentation induced by cAMP protein Fic
META2_0159	147891	148055	165		Cytochrome *c* biogenesis protein, transmembrane region precursor (fragment)
META2_0163	150286	151521	1236		Carbohydrate-selective porin OprB
META2_0168	154237	154971	735		DNA-binding response regulator in two-component regulatory system
META2_0169	154968	156302	1335		Periplasmic sensor signal transduction histidine kinase
META2_0174	159624	162872	3249	*czcA2*	Heavy metal efflux pump CzcA
META2_0176	163478	164395	918	*czcD*	Cation efflux system protein CzcD
META2_0200	179043	179231	189		Cytochrome biogenesis protein (fragment)
META2_0202	180534	181055	522		Signal peptidase II
META2_0203	181052	183247	2196	*zntA*	Zinc, cobalt and lead efflux system
META2_0211	188773	191922	3150	*czcA*	Heavy metal efflux pump CzcA
META2_0214	194332	194544	213	*copP*	CopP metal-binding protein, putative exported protein
META2_0217	196175	199348	3174	*cusA*	Copper/silver efflux system, membrane component
META2_0940	887992	888432	441	*trxC*	Thioredoxin
META2_0962	907338	908885	1548		DNA primase
META2_0971	913402	916275	2874	*polA*	DNA polymerase I
META2_0992	930257	932395	2139	*ligA*	DNA ligase, NAD(+)-dependent
META2_0995	934201	935235	1035	*ruvB*	ATP-dependent DNA helicase, component of RuvABC resolvasome
META2_1007	941539	942450	912		Beta-lactamase domain protein
META2_1009	943278	943727	450		Predicted transporter component
META2_1015	948261	948923	663		DNA-binding response regulator in two-component regulatory system
META2_1016	948920	950236	1317		Integral membrane sensor signal transduction histidine kinase
META2_1021	953252	955546	2295	*katG*	Catalase/hydroperoxidase HPI(I)
META2_1023	956106	957488	1383		Sensor histidine kinase

META2_1024	957481	958158	678		DNA-binding response regulator in two-component regulatory system
META2_1026	959725	962862	3138	*czcA2*	RND divalent metal cation efflux transporter CzcA
META2_1029	963246	963947	702		RNA polymerase ECF-type sigma factor
META2_1058	986951	987994	1044		Tryptophanyl-tRNA synthetase (Tryptophan--tRNA ligase) (TrpRS)
META2_1077	1004463	1004873	411		HNH endonuclease family protein
META2_1083	1010052	1012508	2457	*secA*	Preprotein translocase SecA
META2_tRNA1	1013193	1013282	90		Ser tRNA
META2_1086	1013881	1014990	1110		3'-phosphoadenosine 5'-phosphosulfate sulfotransferase sulfate assimilation)
META2_1098	1027261	1029525	2265		Protein with a domain similar to DNA-directed DNA polymerases
META2_1117	1048329	1049405	1077		Nitrilase
META2_1120	1051831	1052604	774		Nitrilase
META2_1122	1052823	1053830	1008	*qxtB*	Cytochrome bd-quinol oxidase subunit II
META2_1124	1055306	1056532	1227	*hemT*	5-aminolevulinate synthase
META2_1127	1058729	1059643	915	*tehA*	Potassium-tellurite ethidium and proflavin transporter
META2_1128	1059679	1060185	507		Cytochrome *c* family protein
META2_1133	1062849	1063358	510		Ion transport domain protein, C-terminal
META2_1134	1062862	1063626	765		Iron transport domain protein, N-terminal
META2_1135	1063853	1065067	1215	*nhaA*	Sodium-proton antiporter
META2_1141	1068358	1069020	663	*uhpA*	DNA-binding response regulator in two-component regulatory system with UhpB
META2_1190	1100140	1105398	5259		DEAD/DEAH box helicase domain protein
META2_1191	1105395	1108154	2760		Helicase domain protein
META2_1211	1126021	1127037	1017		NADPH quinone oxidoreductase, Zinc-containing alcohol dehydrogenase superfamily
META2_1213	1127541	1128443	903		Transcriptional regulator, LysR family
META2_1218	1131773	1132627	855		Transcriptional regulator, LysR family
META2_1225	1137855	1138760	906		Helix-turn-helix, AraC type:AraC-type transcriptional regulator
META2_1226	1138897	1139640	744		Short-chain dehydrogenase/reductase
META2_1230	1141030	1141839	810	*phnC*	Phosphonate transport protein (ABC superfamily)
META2_1233	1143570	1144589	1020	*ptxD*	Phosphonate dehydrogenase (NAD-dependent phosphite dehydrogenase)
META2_tRNA2	1162482	1162555	74		Gln tRNA
META2_1291	1186946	1187614	669	*rnhB*	Ribonuclease HII, degrades RNA of DNA-RNA hybrids
META2_1296	1189815	1190708	894		Homolog of eukaryotic DNA ligase III
META2_1331	1221864	1225304	3441		Chromosome segregation-like (SMC) protein

* Excluding all hypothetical proteins, putative enzymes, and transposases.

Repeated, selection-driven genome reduction of accessory genome in experimental populations

Ming-Chun Lee,[1] & Christopher J. Marx[1,2,*]

Supporting Information

Text S1

Adaptation in selective environments at generation 1500

Three or four strains were isolated from each population at generation 1500 and their fitness was tested against the fluorescent-labeled ancestor as described in Materials and Methods. The average fitness of each environment was calculated and shown in Figure S1. Overall, the average fitness of evolved populations increased by 15% to 37% in their respective selective environments, indicating the adaptation has occurred in those populations.

Deletion dynamics

By applying the PCR technique as described in methods to the whole population samples at different time points, we found DT1 fixed in 4 populations (B2, B3, B5, B6) before generation 900 and in an additional 9 populations (A1, B1, B4, C3-C8) before generation 1500. We also screened a limited number of available isolates from B populations at generation 480, 540, and 720 (each with ~8 isolates), and found no isolate from generation 480 and 540 had a deletion. However, at generation 720, over 30% of the isolates already had DT1. Interestingly, over 50% of the B isolates had DT2 at this time point, but DT1 was present at generation 1500. The results suggest either DT1 happened in a stepwise fashion, or there might have been multiple genotypes in the population and the multiple DT lineages coexisted due to clonal interference.

Fitness effect and growth rate of deletion mutants

To examine the phenotypic effects of these deletions, we reconstructed four types of compatible deletion mutants (ET1, 2, 3 and 4) (Figure 2A) under the ancestral background by allelic exchange using *sacB* and *cre-lox* systems (1, 2), which let us eliminate the confounding effects of other mutations which occurred along the evolutionary experiment. Figure 2B shows the fitness effects of each of the deletion types across the 4 environments: M, S, MS, and M/S (the average of M→S & S→M). The simplest results were from ET2 where the fitness is slightly beneficial with significant fitness increase of 2 to 4 % in all environments ($P < 0.0001$) except in M→S where significance is marginal ($P = 0.0603$) and from ET3 where the fitness is nearly neutral with increases of 0 to 1% in all environments (P range from 0.01 to 0.0001), indicating ET2 and ET3 are generically either slightly beneficial or neutral across all environments in the ancestral background. We hypothesize,

however, that they may be beneficial in later backgrounds due to epistasis. On the other hand, we found strong environmental specific fitness effects from ET1 and ET4 (Figure 2B). In single substrate environments, substantial fitness increases on S were found both from ET1 (W = 1.145, P < 0.0001) and ET4 (W= 1.107%, P < 0.0001), while the fitness effects on M were rather mild (ET1: W = 1.026, P = 0.0002; ET4: W = 0.984, P = 0.0027) and ET4 is actually deleterious when growing in M-only environment. In the combined-nutrient environments (MS and M/S), we found the fitness of ET1 and ET4 were consistent with the null expectation of being close to the average of the fitness values from the two single-substrate environments (Figure 2B). However, in the alternating environment, there was a substantial fitness decrease on M when transferring from S (~4%, P < 0.0001), but an increased fitness on S when transferring from M (~7%, P < 0.0001), relative to the single substrate environments (Figure 2A). This suggested a substantial effect of the transition between nutrients in both ET1 and ET4. Furthermore, we found the product of fitness values from ET2 and ET4 is very close to the fitness of ET1 across all environments (Figure S2), indicating no deviance in epistasis from independence, such that the transition effect stems from ET4. This result further supports the hypothesis that the region of ET4 was important for nutrient switching.

To get a better understanding of the underlying causes of the fitness changes when switching environments, we performed growth analyses of the engineered deletion mutants. The results revealed a clear discrepancy between the growth rate and fitness values for ET1 and ET4 (Figure S2). In both cases we found the relative growth rates of ET1 and ET4 on either substrate was indistinguishable whether the previous growth cycle was on M or S, indicating growth rate was not the reason for the fitness changes. Due to the limitation on sensitivity of measuring OD_{600} at the low initial values, tracking lag phase itself was fairly inaccurate and did not allow observation of significant differences in the duration of the lag phases between wild type and mutants. However, taking the advantage of the natural diauxic growth observed when *M. extorquens* AM1 switches from S to M, we uncovered a significantly longer transition time from S to M both in ET1 and ET4 (ET1: P = 0.0008; ET4: P = 0.0078) (Figure 2C), which strongly supports the hypothesis of fitness effect of these deletions on nutrient switching. In addition, ET1 and ET4 also exhibited a significantly higher fitness cost during stationary phase (P < 0.0001) (Figure 2D).

The long transition from S to M explains the fitness drop, and the fitness cost at stationary phase might explain the fitness difference between S and M→S in view of the fact that M→S culture experiences shorter stationary phase due to longer lag phase when switching substrates. However, this disadvantage during stationary phase was not due to the survival rate when growing alone. The viable count did not change appreciably (less than 15%) even after 96 hours for all strains (Figure S3). Alternatively, this disadvantage appeared to be due to a small degree of differential cryptic growth during stationary phase.

Gene content

Of the 606 coding sequences in the region of DT1, 415 are annotated as conserved/hypothetical proteins without further informative functions. The major groups of the remaining 191 genes include genes associated with mobile elements, regulatory domains, and stress responses (Table S5). Comparative genomics analysis with two closely related *Methylobacterium extorquens* strains DM4 (NC_012988) (3) and CM4 (NC_011757) also revealed that most of the genes of the megaplasmid are unique to AM1. The only region shared with the other strains of the species is a region around the end of DT1 (Figure 1A) that is present on the chromosome of strain DM4 and CM4, suggesting the potential importance of this region. Interestingly, we found two beta-lactamase family proteins related to ampicillin resistance and one operon related to arsenate resistance located on the region of DT1, although both of them have other homologs on the main chromosome. Moreover, there are 5 sigma factors on the megaplasmid and 3 of them are in the region of DT1. We further performed phylogenetic analysis of those sigma factors along with other sigma factors in the closely related *Methylobacterium* strains and found two of them do not have any homolog in the main chromosome but are conserved in other *Methylobacterium* strains (Figure S5). One of those two sigma factors is a homolog of σ^{24} (or RpoE) and the other is an ECF type sigma factor, which are associated with heat and stress resistance (4). Additionally, we also found 5 genes in the region of DT1 to be induced during phyllosphere colonization (5), suggesting a potential tradeoffs in the ability to associate with plants due to this deletion type. These analyses also revealed a potential replication origin in the region just upstream of DT1, possibly explaining why the boundary of the genome reduction did not extend farther.

Stress responses

Although our data clearly indicate a selective advantage of these deletions under their respective selective conditions, we were interested in extending our phenotypic analysis to investigate the possibility of further tradeoffs in alternative environments (*i.e.*, antagonistic pleiotropy). Our analysis of the gene content lost in the deletions, particularly the ET4 region, pointed to the possibility of altered stress responses. Consistent with the finding of two beta-lactamase family proteins and one operon related to arsenate resistance locating on the region of ET4 (both of them have other homolog genes on the main chromosome), we found that the sensitivity of ET1 and ET4 increased significantly in media with either ampicillin (12.5 μg/mL) (Figure 2E) or arsenate (30mM) (Figure 2F). Finding genes with possible involvement in heat shock (σ^{32} homolog and protein folding/degradation functions) led us to hypothesize deletions of the ET4 region would lead to increased sensitivity to high temperatures. Surprisingly, we found the opposite: a significant improvement on growth rate at 36 °C from ET1 and ET4 (Figure 2G) but the cause of this improvement is still unknown. Other general stresses tested that failed to reveal differences compared to wild-type included: formaldehyde, SDS, peroxide, metal mix, salt, heat shock or UV treatments, as well as all disc diffusion assays. Still, the decrease of antibiotic and heavy metal resistance in liquid medium indicated a tradeoff of this genome reduction.

Lack of epistasis between ET2 and ET4

All phenotypes tested for ET1 and ET4 were qualitatively the same, other than slight differences in the magnitude of effect. This small difference appears to be easily accounted for by including the phenotypic effect of the other half of the large ET1 deletion: ET2. Thus, although the ET1 phenotype is largely due to the ET4 region, the ET1 phenotype could be accounted for by considering each half-deletion to maintain the proportional effect on phenotype that was observed when present alone. The fact that we never found deletions similar to ET4 in the naturally evolved populations and the rare occurrence of DT1 in M/S environment, and the fitness cost during the S→M switch raise suggests that a gene (or genes) within this region contributes to nutrient switching. Furthermore, the fact ET4 was never found in populations despite sometimes being strongly beneficial (e.g., 10% on S) could be due to epistatic interactions with other

mutations that had already occurred within those lines that either reduced or eliminated this selective advantage.

Mutation accumulation

We compared our findings from the evolved populations to those from a series of 10 mutation accumulation populations of the identical *M. extorquens* AM1 transferred through single-colony bottlenecks for 1500 generations. From a total of 10 x 1,500 = 15,000 generations across the populations, no deletions of any type in the region of DT1 were observed. On the other hand, the net rate we observed across the large N_e populations is at least 11.55 per 15,000 generations (37 PCR-detectable deletions across 32 x 1,500 = 48,000 generations assuming the deletions did not occur until exactly 1500 generations). The *P*-value of 0 events in 15, 000 generation under the Poisson distribution of this net rate would be less than 0.0001 by applying the following formula:

$f(k;\lambda) = \frac{\lambda^k e^{-\lambda}}{k!}$, where λ=11.55, and k=0.

The actual difference is even greater, given that the mutations occurred prior to 1500 generations in order to have been observed by then. These data indicate that the observed parallelism here was due primarily, if not exclusively, to selection.

References

1. Marx CJ & Lidstrom ME (2002) Broad-host-range *cre-lox* system for antibiotic marker recycling in gram-negative bacteria. *Biotechniques* 33(5):1062-1067.
2. Marx C (2008) Development of a broad-host-range *sacB*-based vector for unmarked allelic exchange. *BMC Res Notes* 1(1):1.
3. Vuilleumier S*, et al.* (2009) *Methylobacterium* genome sequences: a reference blueprint to investigate microbial metabolism of c1 compounds from natural and industrial sources. *PLoS ONE* 4(5):e5584.
4. Hiratsu K, Amemura M, Nashimoto H, Shinagawa H, & Makino K (1995) The *rpoE* gene of *Escherichia coli*, which encodes sigma E, is essential for bacterial growth at high temperature. *J Bacteriol* 177(10):2918-2922.
5. Gourion B, Rossignol M, & Vorholt JA (2006) A proteomic study of *Methylobacterium extorquens* reveals a response regulator essential for epiphytic growth. *Proc Natl Acad Sci USA* 103(35):13186-13191.